Theory and Practice of Science and Technology
2025, VOL. 6, NO. 3, 16-22
DOI: 10.47297/taposatWSP2633-456903.20250603

COMSOL-based thermal runaway study of firefighting UAV Li-ion battery packs

Xicheng Liu

Paris Elite Institute of Technology, Shanghai Jiao Tong University, Shanghai, 200240, China

ABSTRACT
Firefighting UAVs represent a significant technical apparatus for emergency rescue missions, and as such, they are extensively employed in fire scene reconnaissance and rescue operations due to their high efficiency and flexibility. However, in high-temperature environments, conventional power systems (e.g., lithium battery packs) can significantly affect the range and safety of UAVs due to insufficient heat dissipation performance or poor heat resistance. This paper proposes methods to enhance the heat resistance of Li-ion battery packs employed in high-temperature environments, with the objective of safeguarding the endurance and operational capability of UAVs in extreme conditions. To this end, simulation is carried out by COMSOL software to analyse the thermal runaway behaviour of lithium batteries. The study reveals that the selection of conductor materials significantly impacts the battery pack's heat resistance.

KEYWORDS
UAV; Li-ion battery packs; Thermal runaway; COMSOL

1 Introduction

In recent years, with the acceleration of global urbanisation and the frequent occurrence of extreme weather events caused by climate change, there has been a significant increase in the demand for the response to high-temperature disasters such as forest fires and chemical plant fires. Firefighting drones possess several advantageous characteristics, including comprehensive vision, unmanned operation and flexibility in application. The integration of these unmanned aerial vehicles into the firefighting industry has proven to be a valuable asset, particularly in scenarios involving smoke, high temperatures, and complex fires where access is difficult for firefighters. During rescue operations, firefighters can utilise fire drones to assist with detection, ensuring continuous data collection and facilitating the smooth progression of communication security work. Furthermore, fire drones can transport rescue materials and coordinate the scheduling of rescue teams, enhancing the effectiveness and efficiency of rescue operations and mitigating the risk of significant personnel casualties. [1] However, due to inadequate heat dissipation performance or insufficient heat resistance, the reliability of lithium battery packs in high-temperature environments will be significantly reduced, thereby affecting the endurance and safety of UAVs. Consequently, the subsequent topic that necessitates urgent attention is the enhancement of heat resistance and endurance of Li-ion battery packs.

In the contemporary era, when set against the backdrop of the burgeoning realm of new energy vehicles, the utilisation of firefighting drones equipped with lithium battery packs as power systems remains in its nascent stages. These drones, despite their potential for significant harm in the event of an accident, have not garnered the level of public attention commensurate with their threat potential. However, this does not imply a lack of concern for the issue.2024 On December 12, a drone in Jingzhou, Hubei province, exploded and crashed while in operation, resulting in one individual sustaining severe injuries. The primary causes of fire in lithium battery packs of drones have been identified as follows: overcharging or over-discharging; internal short-circuit; external short-circuit; high-temperature environment; and mechanical damage. However, when discussing firefighting drones, greater emphasis is placed on the lithium battery pack fires caused by the high temperature of the working environment.

In the context of contemporary research endeavours concerning the enhancement of heat-resistance in lithium battery packs within high-temperature environments, there have been several investigations undertaken both domestically and internationally. However, it is evident that the field remains in its nascent stages of development and refinement. In China, with the rapid development of UAV technology, the stability of heat-resistant performance of Li-ion batteries in high-temperature environments has attracted increasing attention as the main power source of UAVs. Wang et al. [2] utilised experimental methodologies to demonstrate that the primary safety concerns associated with lithium batteries stem from thermal runaway phenomena. Consequently, numerous scholars have investigated single batteries from related perspectives. Specifically, Zhen Xiaofei et al. [3] have systematically summarised and analysed the gas generation and diffusion laws during thermal runaway events within lithium battery systems. Furthermore, Wu Juntao et al. [4] investigated the danger of thermal runaway of lithium batteries and combustion trace characteristics. In contrast to earlier research on lithium battery monomers, this paper employs a novel approach by first elucidating the thermal runaway mechanism and then utilising COMSOL to simulate a lithium-ion battery pack. This enables the exploration of the impact of conductor material on thermal performance.

2 Mechanism of thermal runaway

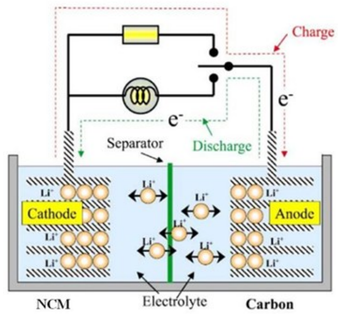

Figure 1 Schematic of the principles of LIB[5]

2.1 Working principles of Li-ion battery

The working principle of a lithium battery is based on the reversible embedding and de-embedding process of lithium ions between the positive and negative electrodes. The specific process can be observed in Figure 1: during the charging cycle, an external power supply applies a voltage, forcing the lithium ions to be de-embedded from the positive electrode material (typically lithium metal oxide, such as LiCoO2) and embedded in the negative electrode material (usually graphite or other carbon-based materials) through the electrolyte and via the diaphragm. Concurrently, the potential difference formed inside leads to the flow of electrons from the positive electrode to the negative electrode through an external circuit, thereby balancing the voltage and forming a current. Conversely, when the battery is being discharged, the reverse of the aforementioned process occurs. The process entails the de-embedding of lithium ions from the negative electrode and their subsequent embedding in the positive electrode, facilitated by the electrolyte via the diaphragm. Concurrently, electrons flow from the negative electrode to the positive electrode through an external circuit. The operating voltage is contingent on the capacity of the positive and negative materials to receive lithium ions; the greater the capacity, the higher the operating voltage. The total reaction equation of discharge is as follows [6], and the discharge reaction is the inverse reaction of charging and is not overly expressed.

$$(Li^0)_x(C^0)_6 \leftrightarrows 6(C^0) + x(Li^+) + xe^-(0 < x < 1) \quad (1)$$

$$(Li^+)_{1-y}(Co^{3+y})(O^{2-})_2 + y(Li^+) + ye^- \leftrightarrows (Li^+)(Co^{3+})(O^{2-})_2 (0 < y < 0.5) \quad (2)$$

2.2 Mechanism of thermal runaway heat generation

In the event of thermal runaway in lithium batteries, a multitude of side reactions are initiated, resulting in the generation of significant heat. This, in turn, accelerates the decomposition of internal materials, thereby inducing a sustained escalation in battery temperature. One battery fails to carry out an uncontrolled chemical exothermic reaction, which in turn triggers a chain reaction, leading to the remaining battery repeating the uncontrolled chemical exothermic reaction. The principle is analogous to the nuclear chain reaction, as illustrated in Figure 2. The primary reactions in this process can be categorised into four distinct types.

2.2.1 SEI membrane (solid electrolyte interface membrane) decomposition reaction

$$R_{sei}(T,C_{sei}) = A_{sei}\exp\left(\frac{-E_{a,sei}}{RT}\right)C_{sei} \quad (3)$$

$$Q_{sei} = H_{sei}W_{sei}R_{sei} \quad (4)$$

$$\frac{dC_{sei}}{dt} = -R_{sei} \quad (5)$$

The following quantities are to be considered:C_{sei} is the dimensionless quantity of the solid electrolyte interphase (SEI) membrane in the stable state;R_{sei} is the reaction parameter of SEI membrane decomposition;A_{sei} is the frequency factor of SEI membrane decomposition; $E_{a,sei}$ is the reaction activation energy of SEI membrane decomposition; H_{sei} is the heat generation rate of SEI membrane decomposition; W_{sei} is the carbon content per unit volume of SEI membrane decomposition.[6]

For example,the following reaction represents the decomposition of lithium alkyl carbonate (ROCO2Li):

$ROCO_2Li \rightarrow Li_2CO_3$+organic matter+heat

The reaction occurs at temperatures ranging from 80°C to 120°C, resulting in the generation of lithium carbonate and organic matter, concurrent with the release of heat. Also, the polymer component of SEI membranes undergoes thermal decomposition at elevated temperatures, generating small molecule gases (e. g. ethylene, methane, etc.) and heat. Furthermore, at elevated temperatures, the components of the SEI membrane may react with solvents in the electrolyte (e.g., ethylene carbonate EC, dimethyl carbonate DMC, etc.) to generate gases and heat.

2.2.2 Negative Electrode and Electrolyte Reaction Graphite reacts with ethylene carbonate (EC)

$$R_{neg}(T,C_{neg}) = A_{neg}exp(-\frac{E_{a,neg}}{RT})C_{neg} \tag{6}$$

$$Q_{neg} = H_{neg}W_{neg}R_{neg} \tag{7}$$

$$\frac{dC_{neg}}{dt} = -R_{neg} \tag{8}$$

The following quantities are to be considered: C_{neg} is the dimensionless quantity of lithium ion content in the carbon layer of the anode; R_{neg} is the reaction parameter of the reaction between the anode and the electrolyte; A_{neg} is the frequency factor of the reaction between the anode and the electrolyte; $E_{a,neg}$ is the reaction activation energy of the reaction between the anode and the electrolyte; H_{neg} is the reaction heating rate of the reaction between the anode and the electrolyte; and W_{neg} is the unit volume of carbon content of the reaction between the anode and the electrolyte.

For example,

C + EC → gas (e.g., ethylene, methane, etc.) + heat

The reaction generates combustible gas (e. g., ethylene, methane, etc.) and heat, which further raises the battery temperature. A reaction between graphite and dimethyl carbonate (DMC) is also observed:

C+DMC→gas (e.g. methanol, carbon dioxide, etc.) + heat

This reaction also releases gas and heat. Finally, the reaction between graphite and lithium hexafluorophosphate (LiPF6) is of note:

$C+LiPF_6 \rightarrow LiF+PF_5$+heat

PF_5 is a strong Lewis acid, which may react further with the solvent in the electrolyte to generate more gas and heat. The gases generated (e.g. ethylene, methane, etc.) may react with other components in the electrolyte or with oxygen to release more heat. For instance, the combustion reaction of ethylene with oxygen is represented by the following equation:

$C_2H_4+3O_2 \rightarrow 2CO_2+2H_2O$+heat.

2.2.3 Reaction of the positive electrode with the electrolyte

$$R_{pos}(T,\alpha) = A_{pos}\alpha(1-\alpha)exp(-\frac{E_{a,pos}}{RT}) \tag{9}$$

$$Q_{pos} = H_{pos}W_{pos}R_{pos} \tag{10}$$

$$\frac{d\alpha}{dt} = -R_{pos} \tag{11}$$

In which the variables are to be considered as: α is the conversion rate of the cathode material involved in the reaction; R_{pos} is the reaction parameter of the cathode-electrolyte reaction; A_{pos} is the frequency factor of the cathode-electrolyte reaction; and $E_{a,pos}$ is the reaction activation energy of cathode-electrolyte reaction; H_{pos} is the reaction heat generation rate of cathode-electrolyte reaction; and W_{pos} is the content of cathode active material per unit volume of cathode-electrolyte reaction.

For instance, we have the reaction of cathode material with lithium hexafluorophosphate (LiPF6) represented by the following equation:

$LiCoO_2+LiPF_6 \rightarrow LiF+PF_5+CoO$+heat

PF_5 is a strong Lewis acid, which may react further with solvents in the electrolyte to generate more gas and heat. Oxygen, released from the decomposition of the anode material, reacts with the solvents in the electrolyte (e.g. EC, DMC, etc.) in a combustion reaction, releasing a significant amount of heat. For instance, the reaction of $C_2H_4O_3$ (EC) with $3O_2$ results in the formation of $2CO_2$, $3H_2O$, and heat.

2.2.4 Electrolyte decomposition reaction

$$R_{ele}(T,C_{ele}) = A_{ele}exp(-\frac{E_{a,ele}}{RT})C_{ele} \tag{12}$$

$$Q_{ele}=H_{ele}W_{ele}R_{ele} \tag{13}$$

$$\frac{dC_{ele}}{dt}=-R_{ele} \tag{14}$$

The following quantities are to be considered: C_{ele} is the dimensionless quantity of electrolyte concentration in the electrolyte; R_{ele} is the reaction parameter of electrolyte decomposition reaction; A_{ele} is the frequency factor of electrolyte decomposition reaction; $E_{a.ele}$ is the reaction activation energy of electrolyte decomposition reaction; H_{ele} is the reaction heat generation rate of electrolyte decomposition reaction; and W_{ele} is the electrolyte content per unit volume of electrolyte decomposition reaction.

For example, there's the process accompanied by the production of carbon dioxide and water, in addition to the release of substantial amounts of heat. A representative example of this reaction is as follows:

$C_3H_4O_3$ (EC) + $3O_2 \rightarrow 3CO_2 + 2H_2O$ + heat.

Table 1 Side reaction parameter values

Parameter	value	unit
H_{sei}	2.570×10^5	J/kg
H_{neg}	1.714×10^5	J/kg
H_{pos}	1.947×10^5	J/kg
H_{ele}	6.200×10^5	J/kg
$E_{a.sei}$	1.38×10^5	J/mol
$E_{a,neg}$	1.32×10^5	J/mol
$E_{a.pos}$	9.90×10^4	J/mol
$E_{a,cle}$	2.70×10^5	J/mol
W_{sei}	1.947×10^5	kgm^3
W_{neg}	220.00	$kg{\cdot}m^3$
W_{pos}	520.000	$kg{\cdot}m^3$
W_{ele}	334.000	$kg{\cdot}m^3$
α_o	0.04	1
A_{sei}	1.66×10^{15}	s^{-1}
A_{neg}	2.50×1013	s-
A_{pos}	2.00×10^3	s^{-1}
A_{ele}	$5.14\times10^2$5	s^{-1}

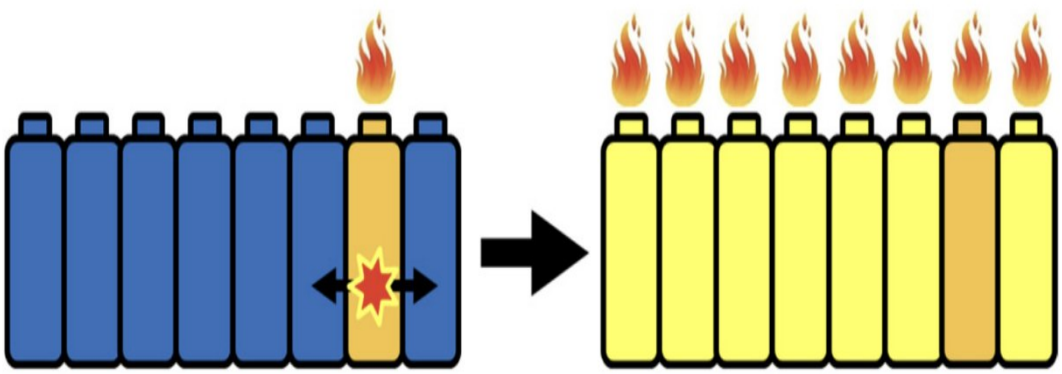

Figure 2 Schematic diagram of the development of thermal runaway in lithium battery packs

3 Model Construction

3.1 Geometric Modeling

A study was conducted to explore the geometric parameters of commercially available 18650 LiPo batteries. The investigation involved the collection of relevant geometric parameters and the execution of geometric modelling using COMSOL, encompassing the battery itself, the bracket, the conductor, and the packaging. The 12S3P battery pack was selected for this study due to the fact that firefighting UAVs typically require high-power battery packs to ensure the successful completion of tasks in extreme environments. The adoption of a cylindrical battery structure is advantageous due to the presence of a gap between the two battery packs, which facilitates effective heat dissipation.Subsequently, the physical parameters of the battery and the environment in the fire scenario are defined, including the battery operating voltage, capacity, ambient temperature, and humidity. The specific data are presented in Figure 3 and table 2.

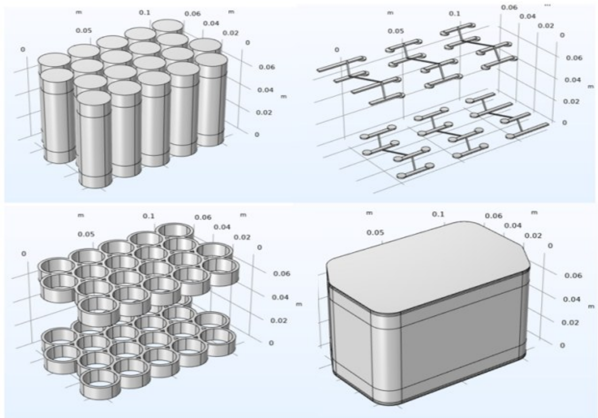

Figure 3 Geometric modeling of lithium battery packs

Table 2 Geometric parameters of lithium battery packs

Description	Value
Diameter of the Battery	0.018 m
Length of the Battery	0.065 m
Holder height	0.01 m
Gap between battery cylinders	0.002 m
Number of series connection	12
Number of parallele connection	3
Battery radius	0.009 m
x displacement for serially connected batteries	0.02 m
y displacement for batteries connected in parallel	0.017321 m
x displacement for batteries connected in parallel	0.01 m
Terminal diameter	0.006 m
Terminal thickness	0.001 m
Serial connector width	0.003 m
Serial connector height	0.001 m
Parallel connector height	0.0005 m
Parallel connector width	0.001 m
Terminal radius	0.003 m

3.2 Thermal runaway modeling

In order to construct a thermal runaway model, it is necessary to consider the known thermal runaway mechanism and the parameters of the lithium battery. The specific data is set out in Table3.

Table 3 Physical parameters of lithium battery pack

Description	Value
Cell capacity	9000 C
Number of battery cells in pack	36
Total 1C pack current (when applied at terminals)	7.5 A
Initial state of charge	0.25
C rate	2
External temperature	303.15 K
Convective cooling heat transfer coefficient	10 W/(m² • K)
Battery in-layer thermal conductivity	30 W/(m • K)
Battery through-layer thermal conductivity	1 W/(m • K)
Battery average density	2000 kg/m³
Battery average heat capacity	1400 J/(kg • K)
Dimensionless charge exchange current density	0.85
Diffusion time constant	1000 s
Ohmic overpotential at 1C	0.0045 V
Trigger temperature for thermal event	353.15 K
Start time for first cell thermal runaway	60 s
Peak time during cell thermal runaway	1 s
Cell thermal runaway time	6 s

4 Simulation experiment analysis

4.1 Electrochemical Performance Analysis

The electrochemical performance of the lithium battery pack is simulated, and the simulation results demonstrate a high degree of consistency with the experiment.The first thermal runaway time is set at 1 min by artificial means, and the voltage change of the battery pack with time during the thermal runaway process is shown in Fig. 4. This is due to the fact that the voltage of the battery pack will reach a maximum of 48.55 V in approximately 3 minutes. The voltage of the battery pack is predicted to reach a maximum of 48.55 V within approximately 3 minutes, attributable to the rise in internal battery temperature and the intensification of the chemical reaction within the battery at the onset of thermal runaway. As the temperature continues to rise, triggering successive thermal runaway events within the battery, the battery resistance increases, electrolyte decomposition occurs, lithium ion exchange capacity diminishes, the current declines, and other factors result in a voltage drop within approximately five minutes, reaching the maximum charging voltage limit and halting the charging process to attain a stable voltage. The variation of the maximum battery temperature with time during the entire thermal runaway process is depicted in Figure 5. The temperature depicted in the figure is representative of the internal battery.

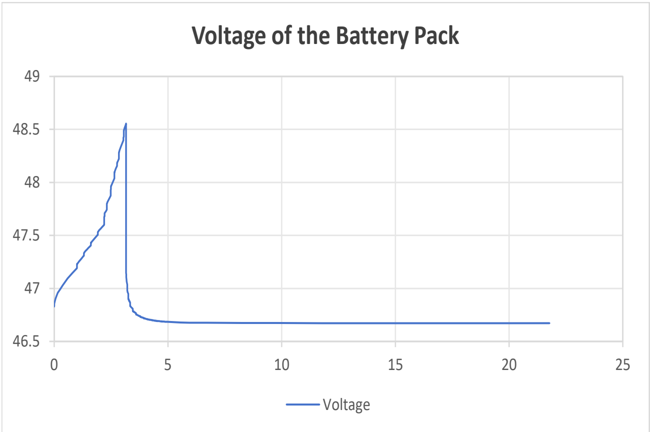

Figure 4 Battery pack voltage during thermal runaway

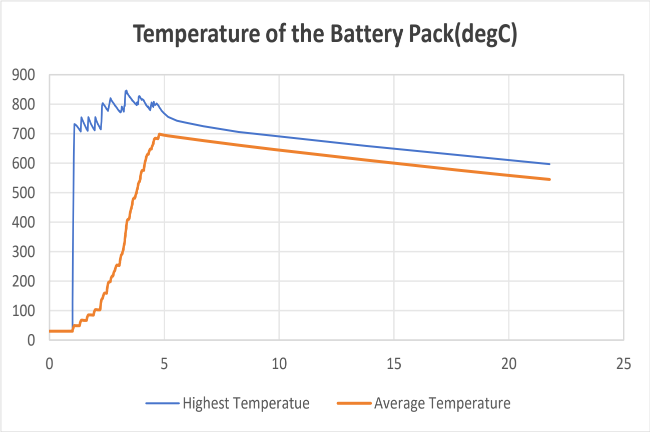

Figure 5 Battery pack temperature during thermal runaway

4.2 Analysis of thermal runaway influencing factors

4.2.1 Environmental temperature effects

The domain differential equations are to be established, with the battery pack being placed under different initial temperature conditions for experimentation at 303.15 K, 333.15 K and 363.15 K. When the internal heat reaches the critical point of the reaction between the cathode material and the electrolyte, a violent side reaction This reaction is characterised by a release of heat that is at least one order of magnitude higher than that of the other side reactions. Consequently, the temperature of the battery pack rises rapidly, leading to uncontrollable conditions. It is noteworthy that the temperature of 1005K is a critical threshold, beyond which the battery pack becomes uncontrollable. Through further experimentation, it has been determined that the temperature at which the thermal runaway of a single lithium battery occurs is approximately 445.08K.

Analytical findings indicate that, in comparison with the heat generated by the ambient temperature, the heat resulting from the internal side reaction of the battery constitutes the primary cause of the thermal runaway of the battery. Consequently, the judicious selection of anode and cathode materials, in conjunction with electrolyte, has the potential to significantly mitigate the risk of thermal runaway.

Furthermore, it has been determined that elevated ambient temperatures result in intensified reactions and accelerated heat release during thermal runaway events within battery packs. Consequently, it is imperative to exercise caution and avoid the prolonged operation of firefighting UAVs in proximity to fire sources.

4.2.2 Effect of heat transfer coefficient

It is important to note that heat transfer is not solely influenced by the ambient temperature; the material of the conductors within the battery pack can also have a significant impact. The generation of heat by these conductors is a primary factor contributing to the thermal runaway of the battery pack. In order to further investigate the impact of different conductor materials on the thermal runaway of the battery pack, the temperature of the battery pack is simulated at the same ambient temperature, using various conductor materials. The study used three distinct conductor materials: AISI4340 steel, copper, and tungsten. The battery pack is configured to undergo thermal runaway within the initial minute, thus focusing on the temperature at which this occurs, while disregarding the duration of the process. The results, as illustrated in Figure 6, indicate that the thermal runaway temperature of the composite conductor battery pack is 732 degrees Celsius, while the thermal runaway temperatures of the copper and tungsten conductors are 768 and 764 degrees Celsius, respectively. This finding aligns with the conclusions drawn from other experiments, which indicate that, at a given temperature, an increase in the heat transfer coefficient leads to an earlier onset of thermal runaway in the battery [7].

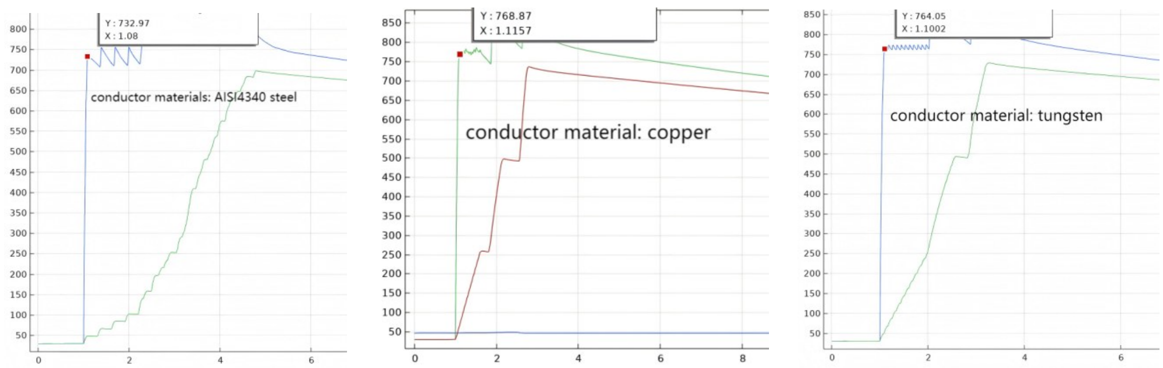

Figure 6 Effect of different conductor materials on thermal runaway temperature

5 Conclusions

The following steps are required to define the thermal runaway process and mechanism of single lithium-ion batteries:

(1)The physical parameters of 18650 lithium batteries must be collected by searching for information or disassembling the objects. Then, a 12-series-3-parallel (12S3P) battery pack model must be constructed in COMSOL.

(2)Analyse the thermal runaway influencing factors from ambient temperature and conductor heat transfer coefficient respectively. Through a series of experiments conducted by the control variable method, it is proved that the risk of thermal runaway will be greatly increased when the lithium-ion battery pack is working for a long time in a high temperature environment. At the same time, the composite conductor material with low thermal conductivity will effectively reduce the risk of thermal runaway of lithium-ion battery packs compared with the pure metal conductor. In order to avoid the occurrence of thermal runaway, it is essential to monitor the temperature inside the lithium battery pack in real time and to stop the drone in time when the critical temperature of thermal runaway is close to the critical temperature or when there is a temperature surge.

(3) In comparison with the heat brought by the environment, the side reaction inside the Li-ion battery pack is the main cause of thermal runaway. Consequently, the judicious selection of positive and negative electrode materials and electrolyte can effectively mitigate the risk of thermal runaway in Li-ion battery packs.

References

[1] Bai, Y., Zhang, S. (2021) Exploration of firefighting drones and their application prospects. Today's Firefighting, 6: 24-25.

[2] WANG, Q., PING, P., ZHAO, X., et al. (2012) Thermal runaway caused fire and explosion of lithium ion battery[J]. Journal of power sources, 208: 210-224.

[3] Zhen, X., Wang, B., Zhang, X., et al. (2024) Study on the generation and diffusion law of thermal runaway gas in lithium battery energy storage system. Energy Storage Science and Technology, 13(6): 1986-1994.

[4] Wu, J., Li, F., Yang, S. (2024) Characterization of thermal runaway hazard and burning traces of 18650 Li-ion ternary battery. Fire Science and Technology, 43(6): 896-901.

[5] Nishi, Y. (2001) The development of lithium ion secondary batteries. Chemical Recouds, 1(5): 406-413

[6] Xu, Y., Liu, J., Cui, B., et al. (2024) Xiao Li's School Adventures: The Working Principles and Safety Risks of Lithium-ion Batteries, 39(9): 259-265.

[7] Yang, M., Yue, L. (2022) COMSOL-based simulation and prevention and control of thermal runaway in lithium-ion batteries, 10(4): 375-382.